



RESEARCH LETTER

10.1002/2015GL064359

Key Points:

- Propose and evaluate a framework that predicts Barents Sea ice cover
- Demonstrate skillful predictions from recent available observations
- Model imperfections can largely be diagnosed from simultaneous meridional winds

Correspondence to:

I. H. Onarheim,
ingrid.onarheim@uib.no

Citation:

Onarheim, I. H., T. Eldevik, M. Årthun, R. B. Ingvaldsen, and L. H. Smedsrud (2015), Skillful prediction of Barents Sea ice cover, *Geophys. Res. Lett.*, *42*, 5364–5371, doi:10.1002/2015GL064359.

Received 24 APR 2015

Accepted 12 JUN 2015

Accepted article online 18 JUN 2015

Published online 8 JUL 2015

©2015. The Authors.

This is an open access article under the terms of the Creative Commons Attribution-NonCommercial-NoDerivs License, which permits use and distribution in any medium, provided the original work is properly cited, the use is non-commercial and no modifications or adaptations are made.

Skillful prediction of Barents Sea ice cover

Ingrid H. Onarheim¹, Tor Eldevik¹, Marius Årthun¹, Randi B. Ingvaldsen², and Lars H. Smedsrud¹

¹Geophysical Institute, University of Bergen and Bjerknes Centre for Climate Research, Bergen, Norway, ²Institute of Marine Research, Bergen, Norway

Abstract A main concern of present climate change is the Arctic sea ice cover. In wintertime, its observed variability is largely carried by the Barents Sea. Here we propose and evaluate a simple quantitative and prognostic framework based on first principles and rooted in observations to predict the annual mean Barents Sea ice cover, which variance is carried by the winter ice (96%). By using observed ocean heat transport and sea ice area, the proposed framework appears skillful and explains 50% of the observed sea ice variance up to 2 years in advance. The qualitative prediction of increase versus decrease in ice cover is correct 88% of the time. Model imperfections can largely be diagnosed from simultaneous meridional winds. The framework and skill are supported by a 60 year simulation from a regional ice-ocean model. We particularly predict that the winter sea ice cover for 2016 will be slightly less than 2015.

1. Introduction

The Arctic sea ice cover is a well-observed and sensitive indicator of climate variability and change [Serreze *et al.*, 2007]. Negative sea ice area trends are observed in all seasons and all regions, but with large seasonal and interannual variability [Cavalieri and Parkinson, 2012; Simmonds, 2015]. The rapid changes in Arctic sea ice cover have led to an increase in demand for realistic local and regional sea ice forecast systems [Eicken, 2013]. Skillful sea ice predictions provide important information for end users interested in marine access, fisheries, and resource extraction, and are also of interest due to the suggested impacts of the Arctic sea ice cover on weather conditions and climate [e.g., Honda *et al.*, 2009; Inoue *et al.*, 2012], although debated [e.g., Screen and Simmonds, 2013; Perlwitz *et al.*, 2014]. The growing effort in producing seasonal to decadal Arctic sea ice forecasts has been especially large for the September minimum sea ice cover [e.g., Schröder *et al.*, 2014; Kapsch *et al.*, 2014; Stroeve *et al.*, 2014]. Predictions of the Arctic winter sea ice variability have on the other hand been limited.

During winter the Arctic Ocean sea ice variability largely reflects variations in the Barents Sea ice cover (Figure 1). An intimate relation between the Barents Sea ice conditions and ocean heat has been understood for more than a century [Helland-Hansen and Nansen, 1909] and was recently quantified by Årthun *et al.* [2012]. Ocean heat anomalies can be generated locally [Schlichtholz, 2011] or be advected from the Norwegian Sea [Vinje, 2001; Kauker *et al.*, 2003; Francis and Hunter, 2007], providing predictive potential for the Barents Sea ice cover. Based on reanalysis data, Nakanowatari *et al.* [2014] found that subsurface temperature has predictive skill for early winter sea ice cover. The influence of the atmosphere on the Barents Sea ice cover has also been highlighted in recent years. Winds affect the Barents Sea climate variability through transport and redistribution of sea ice [Hilmer *et al.*, 1998; Koenig *et al.*, 2009; Kwok, 2009], advection of air masses and Atlantic heat into the Barents Sea [Ingvaldsen *et al.*, 2004a; Kvingedal, 2005], and by increasing turbulent surface heat fluxes. The largest influence of northerly winds is often found during winter due to stronger winds [Pavlova *et al.*, 2013]. Processes related to large-scale atmospheric circulation [Maslanik *et al.*, 2007; Deser and Teng, 2008; Zhang *et al.*, 2008], cyclone activity [Sorteberg and Kvingedal, 2006; Simmonds and Keay, 2009], the length of the freezing season, and the amount of ice that remains after the summer melt season may also be of large importance for the sea ice variability.

The aim of this study is to understand and assess the predictability of the annual mean, and, in particular, the winter Barents Sea ice cover (Figure 1). We develop a prognostic framework from first principles and, based on direct observations and a 60 year simulation, assess the role of the Atlantic inflow as a main source of Barents Sea ice predictability 1–2 years in advance. Moreover, the influence and predictive potential of meridional winds on the interannual sea ice variability are investigated.

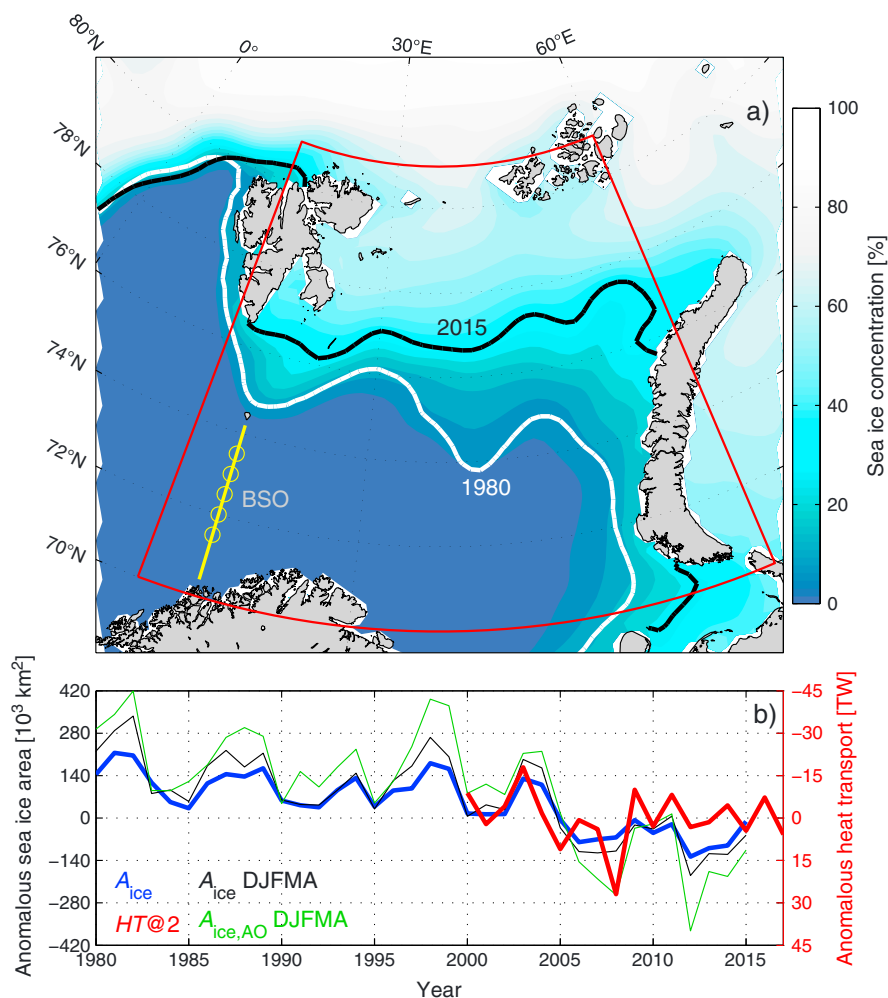


Figure 1. (a) Satellite-derived (National Snow and Ice Data Center, NSIDC) mean sea ice concentration between 1980 and 2015. The ice edge (15% ice concentration) is indicated for 1980 (white line) and 2015 (black line). We confine the Barents Sea by the red line. The mooring array across the Barents Sea Opening (BSO, yellow line) is indicated by yellow circles. (b) Time series of interannual sea ice area. Annual (July–June, blue) sea ice variability is dominated by changes in winter (December–April, black) sea ice area. During winter variations in the anomalous Arctic Ocean (interior basins and surrounding shelf seas) sea ice area (green) mainly reflect the Barents Sea ice variability; the correlation between the winter sea ice area in the Barents Sea and the Arctic Ocean is 0.96, and the standard deviations are $131 \cdot 10^3 \text{ km}^2$ and $191 \cdot 10^3 \text{ km}^2$, respectively. Observed annual mean heat transport (red) shifted to the ice cover by 2 years is also shown (note reversed axis).

2. Data and Methods

We confine the Barents Sea to the area between 70–81°N, 15–60°E (Figure 1; following *Árthun et al.* [2012]). The Barents Sea ice cover is characterized by a strong seasonal cycle where almost all ice melts in summer. The majority of sea ice is formed locally during winter [e.g., *Vinje*, 2001], although in some winters sea ice import from the Arctic Ocean is substantial [*Kwok et al.*, 2005]. We thus consider winter-centered annual means (July–June) for all variables, i.e., the indicated year denotes the winter-centered mean that ends in the respective year (e.g., 2015 represents July 2014 to June 2015). As the summer is practically ice free, winter (December–April) explains 96% of the annual mean variance.

2.1. Observations

Monthly sea ice area from 1979 to 2015 is obtained from the National Snow and Ice Data Center (NSIDC) [*Cavalieri et al.*, 1996], with a spatial resolution of $25 \text{ km} \times 25 \text{ km}$. The sea ice algorithms and the method used to derive a consistent data set are described in *Cavalieri et al.* [1999, and references therein].

To test the Atlantic heat transport as a potential predictor of the Barents Sea ice cover, we use the Atlantic water ($T > 3^{\circ}\text{C}$) [Ingvaldsen *et al.*, 2004b] inflow through the Barents Sea Opening (BSO, $71.5\text{--}73.5^{\circ}\text{N}$, 20°E), measured by the Institute of Marine Research, Norway since September 1997. Current meter moorings deployed every 30 nm (= 56 km) in the BSO sample temperature and velocity at 50 m depth and 15 m above bottom (the current is mostly barotropic, driven by sea level changes [Ingvaldsen *et al.*, 2004a]), allowing for calculation of heat transport. July and August 1997, and May and June 2015 are estimated from climatological (1998–2014) values in order to get winter-centered annual mean values for 1998 and 2015, respectively. Note that the near-real-time data from April 2014 to April 2015 was postprocessed in the field after recovering the moorings. The 2015 value used herein is therefore a present best estimate of recent heat transport.

The influence from regional winds on the sea ice variability is investigated using monthly reanalysis data of the meridional wind component from the National Centers for Environmental Prediction (NCEP)-National Centers for Atmospheric Research (NCAR) [Kalnay *et al.*, 1996] on a $2.5^{\circ} \times 2.5^{\circ}$ grid. The reanalysis data are comparable to observed surface wind speeds over the Barents Sea [Kolstad, 2008] and capture synoptic changes in sea level pressure distribution and associated changes in geostrophic winds [e.g., Deser and Teng, 2008].

2.2. Model Simulation

To complement the relatively short observational record, we use the 60 year (1948–2007) model simulation of Årthun *et al.* [2011]. The model used is the regional coupled ice-ocean model Hamburg Shelf Ocean Model (HAMSOM) [Schrum and Backhaus, 1999]. HAMSOM has a horizontal resolution of $7\text{km} \times 7\text{ km}$ and is forced with NCEP/NCAR reanalysis data. The model shows good agreement with observations, in general, and in particular with the Barents Sea ice area [Årthun *et al.*, 2012]; the simulated sea ice area is essentially the observed. The hydrographic structure of the Barents Sea is also captured by the model, and the interannual variability is realistic. Accordingly, the HAMSOM simulation seems appropriate to examine the predictability of the Barents Sea ice cover.

2.3. Prediction Evaluation

Prediction skill is assessed by variance explained (r^2), and root-mean-square error, $\text{RMSE} = \left[\sum_{i=1}^N (x_i - y_i)^2 / N \right]^{1/2}$, where N is the length of the time series and x and y are the observed and predicted time series, respectively. A common definition of skill is for a prediction framework to beat persistence [e.g., Kapsch *et al.*, 2014]. The persistence forecast is simply constructed by assuming that the present rate of change in sea ice area persists. Predicted change is quantified with respect to the presently observed sea ice area. They are both scored against the sign of change subsequently observed. The proposed framework is also evaluated against linear trend predictions, which are constructed by extrapolating the observed linear trend in sea ice cover. The term skillful herein describes a prediction that beats the skill both of persistence and of linear trend prediction.

3. Prognostic Framework

The Barents Sea is a confined, relatively shallow basin where the oceanic heat is essentially provided through the BSO [e.g., Smedsrud *et al.*, 2013], and effectively lost to the atmosphere in the southern ice-free part [Häkkinen and Cavalieri, 1989; Årthun and Schrum, 2010; Smedsrud *et al.*, 2010]. Consequently, there is little heat leaving the Barents Sea to the Arctic Ocean [Gammelsrød *et al.*, 2009]. Both the recent trend and the sea ice variability are largely related to the inflowing Atlantic water through the BSO [Årthun *et al.*, 2012]. We now outline a predictive and explicit framework linking ocean heat transport to the Barents Sea ice cover.

The integrated heat budget of the Barents Sea is

$$\frac{dHC}{dt} = -HF + HT, \tag{1}$$

with HC being the ocean heat content, HF the net surface heat flux (the sum of shortwave, longwave, sensible, and latent heat fluxes at the ocean surface), and HT the ocean heat transport through the BSO. The quantities will be understood as anomalies for the present application. An increase in heat transport through the BSO results in warmer ocean conditions, larger heat loss to the atmosphere, and hence reduced sea ice freezing and smaller sea ice cover. Årthun *et al.* [2012] found that the regional ocean heat content and heat loss to the atmosphere reflect the annual mean extent of ice-free ocean. Hence, we model the anomalous ocean heat content and heat loss to the atmosphere to scale with the anomalous sea ice area, A_{ice} :

$$HC = -hc_0 A_{\text{ice}}, \quad HF = -q_0 A_{\text{ice}}, \tag{2}$$

where hc_0 and q_0 are scaling factors representing the heat content and heat loss per area of an anomalous ice-free sea surface (see Appendix A for details). Inserting the scaling into the conservation of heat results in a simple prognostic relation for the anomalous sea ice area, where heat loss to the atmosphere acts as a relaxation toward no anomalous sea ice area, and ocean heat transport drives changes in sea ice area:

$$\frac{dA_{\text{ice}}}{dt} = -\frac{q_0}{hc_0}A_{\text{ice}} - \frac{1}{hc_0}HT. \quad (3)$$

The relation constitutes a quantification of changes in the sea ice area from ocean heat transport and sea ice area. In its simplest form, the right-hand side represents a qualitative prediction for the sign of change from which is the most dominant predictor, ice cover versus heat transport. Hence, the framework predicts the Barents Sea ice area based on observed sea ice area and heat transport through the BSO.

Solving equation (3) analytically results in an explicit expression of the anomalous sea ice area:

$$A_{\text{ice}}(t) = \left(A_0 - \frac{1}{q_0\tau} \int_0^t HT(t)e^{\frac{t}{\tau}} dt \right) e^{-\frac{t}{\tau}}, \quad (4)$$

where A_0 is the initial sea ice anomaly and $\tau = hc_0/q_0$ is the characteristic time scale for heat balance indicating the flushing time of the Barents Sea. The anomalous sea ice area at a given time is thus set by the initial sea ice area and the integrated heat input through the BSO. The weight of the past decreases exponentially with time scale τ . Both the observational record and the HAMSOM data indicate a memory (heat balance) of the Barents Sea of approximately 3 years (Appendix A). This compares well with the flushing time of the Barents Sea which is less than 5 years based on a throughflow of 2 Sv ($1\text{ Sv} = 10^6 \text{ m}^3 \text{ s}^{-1}$) and a basin volume of $3 \cdot 10^{14} \text{ m}^3$ and is also consistent with the lagged sea ice response to a variable Atlantic inflow, as suggested by *Arthur et al.* [2012].

Forward discretization of equation (3) gives a prognostic relation linking the anomalous sea ice area to the anomalous ice area and heat transport the previous year:

$$A_{\text{ice}}^{n+1} = -\left(\frac{q_0}{hc_0}A_{\text{ice}}^n + \frac{1}{hc_0}HT^n \right) \Delta t + A_{\text{ice}}^n, \quad (5)$$

where n indicates time and Δt is the time step of 1 year. Note that equation (5) predicts year $n + 1$ based on the true sea ice area and heat transport for year n , i.e., a simplest form of data assimilation. Equation (4) integrates the heat transport over time only considering the initial sea ice anomaly. Hence, the analytical solution in equation (4) potentially accumulates model imperfections (related to equation (2)) with time. Predictions based on the discretized equation (5) can therefore maybe be expected to be more skillful, and to be more appropriate for practical use.

4. Predictions of the Barents Sea Ice Cover

To evaluate the proposed framework predicting the Barents Sea ice cover, we first use direct observations and thereafter the 60 year model simulation. Using the observation-based scaling parameters (cf. Appendix A) in equations (4) and (5) allows for predictions of the Barents Sea ice cover based on available observations. The analytical estimate using direct observations as input shows good agreement to the observed sea ice cover (Figure 2a). Using equation (5), 50% of the variance is explained, and the RMSE is relatively small (roughly half of a standard deviation of $91 \cdot 10^3 \text{ km}^2$; Table 1). There is, however, the expected underestimation of magnitude due to variance not explained (cf. Appendix A). This suggests that the proposed framework linking observed Barents Sea ice cover and heat transport through the BSO is useful for predicting the Barents Sea ice cover 1 year in advance. It is in particular predicted that the sea ice area in 2016 will be $12 \cdot 10^3 \text{ km}^2$ smaller than that of 2015. The predicted sea ice area for 2016 is near the mean over the last 20 years, but still corresponds to the eighth lowest sea ice area since 1979. The results are supported by HAMSOM data (Figure 2b). Based on equation (4), the analytical estimate using HAMSOM data as input explains 63% of the variance in sea ice cover, and the RMSE is relatively small ($43 \cdot 10^3 \text{ km}^2$ compared to the standard deviation of $69 \cdot 10^3 \text{ km}^2$). For HAMSOM the prediction from the integral equation (4) is slightly better than the prediction based on equation (5), with $r^2 = 55\%$ and $\text{RMSE} = 46 \cdot 10^3 \text{ km}^2$. This corroborates that ocean heat transport is a dominant driver of the HAMSOM simulated sea ice cover.

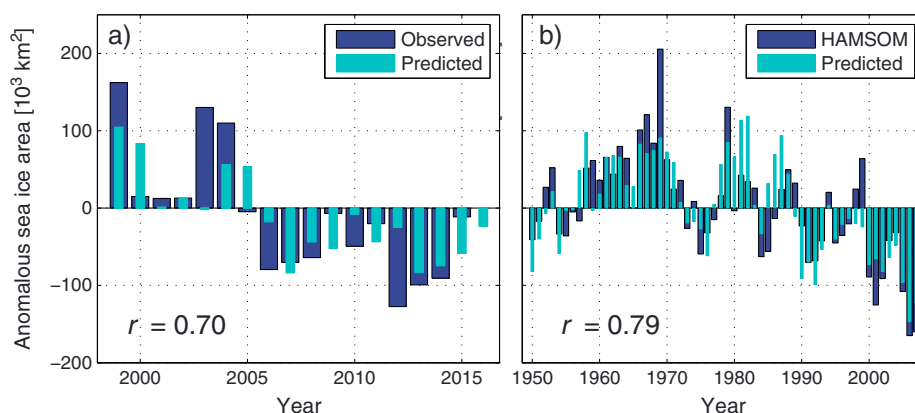


Figure 2. (a) Annual (July–June) observed and predicted anomalous Barents Sea ice area between 1999 and 2016. Anomalies are relative to the mean sea ice area of $238 \cdot 10^3 \text{ km}^2$ for the 1998–2015 period. The prediction is based on the sea ice area and heat transport through the Barents Sea Opening the previous year (equation (5)). (b) Annual (July–June) modeled (HAMSOM) and predicted anomalous Barents Sea ice area between 1950 and 2007. Anomalies are relative to the mean sea ice area of $377 \cdot 10^3 \text{ km}^2$ for the 1949–2007 period. The prediction is based on the integrated heat transport through the Barents Sea Opening and the initial sea ice area (equation (4)).

5. Evaluation of Predictability

As our prediction of the Barents Sea ice cover compares well with observed sea ice variability, we now assess the skill (cf. section 2) of the proposed framework. The qualitative prediction of an increase/decrease in sea ice cover is correct in 15 years out of the 17 available years, i.e., 88% of the time considering the observations retrospectively (Figure 3 and Appendix A). The proposed method to predict changes in sea ice cover thus beats persistence (correct 88% of the time compared to 63% for persistence). Our physically based framework also beats linear trend predictions. By considering the trend over the period of observed heat transport, the linear trend prediction gives a RMSE of $87 \cdot 10^3 \text{ km}^2$, compared with $56 \cdot 10^3 \text{ km}^2$ from equation (5) (Table 1). The RMSE is slightly reduced ($73 \cdot 10^3 \text{ km}^2$) when basing extrapolation on the full satellite observed sea ice record. We thus find the proposed framework to be skillful.

To further evaluate the framework, we account for the memory of the Barents Sea (3 years; Appendix A), and evaluate the prediction with up to 3 years time lag between heat transport and sea ice cover. Accordingly the forecast horizon of the framework may possibly be extended. Results from linear regression (cf. equation (A1)) show that the observational based prediction is slightly improved using a 2 year leading heat transport (Table 1). The heat transport leading the ice cover by 3 years has only a minor influence on the sea ice cover. The forecast horizon can thus be considered to be to 2 years from the point of view of ocean heat transport.

Table 1. Evaluation Statistics for the Predictions^a

Method	Observations		HAMSOM	
	r^2	RMSE	r^2	RMSE
Based on equation (5)				
$A_{ice@1, HT@1}$	50	56	55	46
$A_{ice@1, HT@2}$	50	49	41	53
$A_{ice@1, HT@1, v@1}$	52	55	63	42
$A_{ice@1, HT@1, v@0}$	78	38	66	40
Based on equation (4)				
	42	69	63	43

^aExplained variance, r^2 (%); root-mean-square error, RMSE ($\times 10^3 \text{ km}^2$); and time lag, @ (year). A_{ice} , sea ice area; HT , ocean heat transport; and v , meridional wind; all are anomalies.

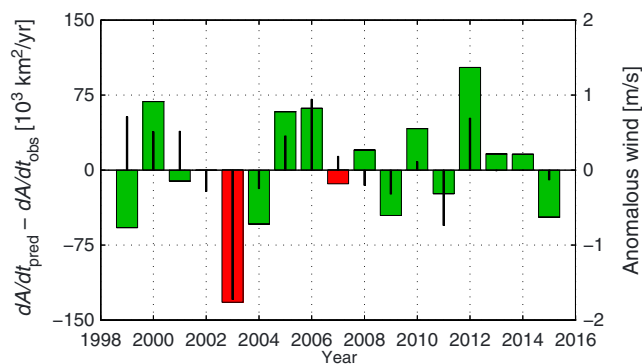


Figure 3. Difference between predicted and observed rate of change in the Barents Sea ice cover from one year to the next (thick bars). Green indicates that the correct sign of change is predicted and red the opposite. Thin bars show anomalous wind (meridional wind component averaged over the Barents Sea), where positive values indicate wind from the south.

Our suggested framework has so far not considered wind explicitly. Winds may have a large impact on interannual sea ice variability [e.g., Kwok, 2009] and was suggested as a possible predictor by *Nakanowatari et al.* [2014]. Our large underestimation of sea ice in 2003 corresponds to anomalous winds from the north (Figure 3). According to *Kwok et al.* [2005] winds caused an unusually high import of sea ice to the Barents Sea during winter 2003. Due to the potential influence of winds, we examine meridional wind at different time lags as predictor. Using linear regression analysis (cf. equation (A1)), we find that the prediction performance is not largely improved by accounting for wind with a time lag, while simultaneous wind adds variance explained (Table 1), consistent with the findings of *Nakanowatari et al.* [2014]. The effect from simultaneous wind is demonstrated in Figure 3, showing that mismatch between observed and predicted changes in the ice cover can be reconciled also considering anomalous wind conditions. By combining the predictive equation (5) with simultaneous winds (in the form of equation (A1)), 78% of the sea ice variance is explained (Table 1). A more elaborate evaluation of wind influence, by investigating more regional winds, indicates that the results are robust. This corroborates that ocean heat conditions and winds appear as main drivers of the Barents Sea ice cover. Still, the proposed framework (equation (4) or (5)) captures most of the sea ice variance and qualitatively predicts an increase/decrease in ice cover skillfully.

6. Discussion and Conclusion

Using direct observations, a regional ice-ocean model and a simple prognostic heat budget (equations (1)–(5)), we have shown that sea ice anomalies in the Barents Sea can be skillfully predicted from recent sea ice area and ocean heat transport. Overall the proposed framework skillfully predicts the observed sea ice cover both quantitatively (Figure 2) and qualitatively (Figure 3) predicting an increase versus decrease in ice cover. By accounting for simultaneous meridional winds, 78% of the sea ice variance is explained. Preceding ocean heat transport and sea ice area combined with these winds are thus all important to explain recent sea ice variability (Table 1).

As ocean heat transport and sea ice cover provide significant predictive skill for the Barents Sea ice cover, this work corroborates the strong link between Atlantic water inflow and the Barents Sea ice cover [e.g., *Schlichtholz*, 2011; *Årthun et al.*, 2012]. *Parkinson et al.* [2006] found that many climate models simulate more sea ice in the Barents Sea than what is observed and hypothesized that the models underestimate the ocean heat transport. It thus appears essential for ocean and earth system models to adequately resolve the variable Atlantic heat transport through the Nordic Seas into the Barents Sea and Arctic Ocean, in order to simulate Arctic sea ice variability well.

The proposed framework offers a novel approach to predict winter Arctic sea ice cover, where the Barents Sea at present essentially explains the winter variance (92%, cf. Figure 1b). Related to this, *Zhang* [2015] suggested a relation between the Barents Sea ice cover and also summer Arctic sea ice extent via Atlantic heat. Skillful predictions of Barents Sea ice may therefore have the potential to improve predictions of the Arctic Ocean sea ice cover in general. In the future the processes driving today's Barents Sea winter ice cover may become even more relevant as first-year ice is likely to dominate the Arctic Ocean.

Our results highlight the potential for skillful physical-based prediction models of the Arctic sea ice cover. We demonstrate that the Barents Sea ice cover is skillfully predictable 1–2 years ahead (Figure 2). Due to relatively small 2015 anomalies in sea ice and heat, but with a relative dominance of anomalous Atlantic heat input, it is in particular predicted (cf. equation (5)) that the Barents Sea ice cover in 2016 will be smaller than that of 2015 (Figure 2a).

Appendix A: Scaling Parameters

Our suggested framework (equation (5)) can be considered a special case of the regressional relation

$$\frac{A_{\text{ice}}^{n+1} - A_{\text{ice}}^n}{\Delta t} = aA_{\text{ice}}^{n-k} + bHT^{n-l} + c\nu^{n-m}, \quad (\text{A1})$$

where a , b , and c are regression coefficients for the ice cover, heat transport, and meridional wind, ν , respectively, and k , l , m are any additional time lags. In the case of equation (5), $c = k = l = 0$, i.e., neither the direct influence of wind nor any time lag beyond the present are considered, and $a = -q_0/hc_0$, $b = -1/hc_0$. Simplest estimates of the scaling factors, q_0 and hc_0 , would be $hc_0 = \text{std}(HC)/\text{std}(A_{\text{ice}})$ and $q_0 = \text{std}(HF)/\text{std}(A_{\text{ice}})$, where $\text{std}(X)$ is the standard deviation of the annual time series X , and assuming the model assumption (equation (2)) to be perfect. Unfortunately, observational time series of ocean heat content and heat flux to the atmosphere are not available. By considering the full observational record, linear regression (equation (A1)) gives $a = -0.403 \text{ yr}^{-1}$, and $b = -0.001 \text{ m}^2 \text{ J}^{-1}$ for the observational record. For HAMSO data the regression coefficients become $a = -0.617 \text{ yr}^{-1}$ and $b = -0.003 \text{ m}^2 \text{ J}^{-1}$, which compare well with scaling parameters calculated from standard deviations ($a = -0.616 \text{ yr}^{-1}$ and $b = -0.005 \text{ m}^2 \text{ J}^{-1}$). The observed and modeled parameters differ partly because the scaling parameters may change over time but also simply because HAMSO is a model. The robustness of the scaling parameters was therefore tested by the random subsampling of N data points for the regressional relationship (equation (A1); $N \leq 30$ for HAMSO; $N \leq 12$ for observations). The procedure was repeated 1000 times for each N . The scaling parameters converged to their respective values in about 15 years, implying the HAMSO estimates to be robust, but that one would probably still benefit from a longer observational series. We finally note that prediction based on regression generically underestimates the variance of a predictand unless there is perfect covariance between predictor(s) and the predictand (cf. Figure 2).

Acknowledgments

The data sets for this paper are properly cited and referred to in the reference list. This work was supported by the Centre for Climate Dynamics (SKD) at the Bjerknes Centre and by the Research Council of Norway through the projects NORTH and EPOCASA. We thank two anonymous reviewers for constructive suggestions that improved the manuscript.

The Editor thanks two anonymous reviewers for their assistance in evaluating this paper.

References

- Årthun, M., and C. Schrum (2010), Ocean surface heat flux variability in the Barents Sea, *J. Mar. Syst.*, *83*, 88–98, doi:10.1016/j.jmarsys.2010.07.003.
- Årthun, M., R. B. Ingvaldsen, L. H. Smedsrud, and C. Schrum (2011), Dense water formation and circulation in the Barents Sea, *Deep Sea Res.*, *58*(8), 801–817, doi:10.1016/j.dsr.2011.06.001.
- Årthun, M., T. Eldevik, L. H. Smedsrud, Ø. Skagseth, and R. B. Ingvaldsen (2012), Quantifying the influence of Atlantic heat on Barents Sea ice variability and retreat, *J. Clim.*, *25*, 4736–4743, doi:10.1175/JCLI-D-11-00466.1.
- Cavalieri, D. J., and C. L. Parkinson (2012), Arctic sea ice variability and trends, 1979–2010, *Cryosphere*, *6*(4), 881–889, doi:10.5194/tc-6-881-2012.
- Cavalieri, D. J., C. L. Parkinson, P. Gloersen, and H. Zwally (1996), *Sea Ice Concentrations From Nimbus-7 SMMR and DMSP SSM/I Passive Microwave Data*, Digital Media, Natl. Snow and Ice Data Cent., Boulder, Colo.
- Cavalieri, D. J., C. L. Parkinson, P. Gloersen, J. C. Comiso, and H. J. Zwally (1999), Deriving long-term time series of sea ice cover from satellite passive-microwave multisensor data sets, *J. Geophys. Res.*, *104*(C7), 15,803–15,814, doi:10.1029/1999JC900081.
- Deser, C., and H. Teng (2008), Evolution of Arctic sea ice concentration trends and the role of atmospheric circulation forcing, 1979–2007, *Geophys. Res. Lett.*, *35*, L02504, doi:10.1029/2007GL032023.
- Eicken, H. (2013), Ocean science: Arctic sea ice needs better forecasts, *Nature*, *497*(7450), 431–433, doi:10.1038/497431a.
- Francis, J. A., and E. Hunter (2007), Drivers of declining sea ice in the Arctic winter: A tale of two seas, *Geophys. Res. Lett.*, *34*, L17503, doi:10.1029/2007GL030995.
- Gammelsrød, T., Ø. Leikvin, V. Lien, W. P. Budgell, H. Loeng, and W. Maslowski (2009), Mass and heat transports in the NE Barents Sea: Observations and models, *J. Mar. Syst.*, *75*(1), 56–69, doi:10.1016/j.jmarsys.2008.07.010.
- Häkkinen, S., and D. J. Cavalieri (1989), A study of oceanic surface heat fluxes in the Greenland, Norwegian, and Barents Seas, *J. Geophys. Res.*, *94*(C5), 6145–6157, doi:10.1029/JC094iC05p06145.
- Helland-Hansen, B., and F. Nansen (1909), The Norwegian Sea, *Fiskdir. Skr. Ser. Havunders.*, *2*(2), 1–360.
- Hilmer, M., M. Harder, and P. Lemke (1998), Sea ice transport: A highly variable link between Arctic and North Atlantic, *Geophys. Res. Lett.*, *25*(17), 3359–3362, doi:10.1029/98GL52360.
- Honda, M., J. Inoue, and S. Yamane (2009), Influence of low Arctic sea-ice minima on anomalously cold Eurasian winters, *Geophys. Res. Lett.*, *36*, L08707, doi:10.1029/2008GL037079.
- Ingvaldsen, R. B., L. Asplin, and H. Loeng (2004a), Velocity field of the western entrance to the Barents Sea, *J. Geophys. Res.*, *109*, C03021, doi:10.1029/2003JC001811.
- Ingvaldsen, R. B., L. Asplin, and H. Loeng (2004b), The seasonal cycle in the Atlantic transport to the Barents Sea during the years 1997–2001, *Cont. Shelf Res.*, *24*(9), 1015–1032, doi:10.1016/j.csr.2004.02.011.

- Inoue, J., M. E. Hori, and K. Takaya (2012), The role of Barents Sea ice in the wintertime cyclone track and emergence of a warm-Arctic cold-Siberian anomaly, *J. Clim.*, *25*(7), 2561–2568, doi:10.1175/JCLI-D-11-00449.1.
- Kalnay, E., et al. (1996), The NCEP/NCAR 40-year reanalysis project, *Bull. Am. Meteorol. Soc.*, *77*(3), 437–471, doi:10.1175/1520-0477(1996)077<0437:TNYRP>2.0.CO;2.
- Kapsch, M.-L., R. G. Graversen, T. Economou, and M. Tjernström (2014), The importance of spring atmospheric conditions for predictions of the Arctic summer sea ice extent, *Geophys. Res. Lett.*, *41*, 5288–5296, doi:10.1002/2014GL060826.
- Kauker, F., R. Gerdes, M. Karcher, C. Köberle, and J. L. Lieser (2003), Variability of Arctic and North Atlantic sea ice: A combined analysis of model results and observations from 1978 to 2001, *J. Geophys. Res.*, *108*(C6), 3182, doi:10.1029/2002JC001573.
- Koenigk, T., U. Mikolajewicz, J. H. Jungclaus, and A. Kroll (2009), Sea ice in the Barents Sea: Seasonal to interannual variability and climate feedbacks in a global coupled model, *Clim. Dyn.*, *32*(7–8), 1119–1138, doi:10.1007/s00382-008-0450-2.
- Kolstad, E. (2008), A QuikSCAT climatology of ocean surface winds in the Nordic seas: Identification of features and comparison with the NCEP/NCAR reanalysis, *J. Geophys. Res.*, *113*, D11106, doi:10.1029/2007JD008918.
- Kvingedal, B. (2005), Sea-ice extent and variability in the Nordic Seas, 1967–2002, in *The Nordic Seas: An Integrated Perspective*, vol. 158, edited by B. Kvingedal, pp. 137–156, AGU, Washington, D. C., doi:10.1029/158GM04.
- Kwok, R. (2009), Outflow of Arctic Ocean sea ice into the Greenland and Barents Seas: 1979–2007, *J. Clim.*, *22*(9), 2438–2457, doi:10.1175/2008JCLI2819.1.
- Kwok, R., W. Maslowski, and S. W. Laxon (2005), On large outflows of Arctic sea ice into the Barents Sea, *Geophys. Res. Lett.*, *32*, L22503, doi:10.1029/2005GL024485.
- Maslanik, J., S. Drobot, C. Fowler, W. Emery, and R. Barry (2007), On the Arctic climate paradox and the continuing role of atmospheric circulation in affecting sea ice conditions, *Geophys. Res. Lett.*, *34*, L03711, doi:10.1029/2006GL028269.
- Nakanowatari, T., K. Sato, and J. Inoue (2014), Predictability of the Barents Sea ice in early winter: Remote effects of oceanic and atmospheric thermal conditions from the North Atlantic, *J. Clim.*, *27*(23), 8884–8901, doi:10.1175/JCLI-D-14-00125.1.
- Parkinson, C. L., K. Y. Vinnikov, and D. J. Cavalieri (2006), Evaluation of the simulation of the annual cycle of Arctic and Antarctic sea ice coverages by 11 major global climate models, *J. Geophys. Res.*, *111*, C07012, doi:10.1029/2005JC003408.
- Pavlova, O., V. Pavlov, and S. Gerland (2013), The impact of winds and sea surface temperatures on the Barents Sea ice extent, a statistical approach, *J. Mar. Syst.*, *130*, 248–255, doi:10.1016/j.jmarsys.2013.02.011.
- Perlwitz, J., M. Hoerling, and R. Dole (2014), Arctic tropospheric warming: Causes and linkages to lower latitudes, *J. Clim.*, *28*, 2154–2167, doi:10.1175/JCLI-D-14-00095.1.
- Schlichtholz, P. (2011), Influence of oceanic heat variability on sea ice anomalies in the Nordic Seas, *Geophys. Res. Lett.*, *38*, L05705, doi:10.1029/2010GL045894.
- Schröder, D., D. L. Feltham, D. Flocco, and M. Tsamados (2014), September Arctic sea-ice minimum predicted by spring melt-pond fraction, *Nat. Clim. Change*, *4*(5), 353–357, doi:10.1038/nclimate2203.
- Schrum, C., and J. O. Backhaus (1999), Sensitivity of atmosphere-ocean heat exchange and heat content in the North Sea and the Baltic Sea, *Tellus A*, *51*(4), 526–549, doi:10.1034/j.1600-0870.1992.00006.x.
- Screen, J. A., and I. Simmonds (2013), Exploring links between Arctic amplification and mid-latitude weather, *Geophys. Res. Lett.*, *40*, 959–964, doi:10.1002/grl.50174.
- Serreze, M. C., M. M. Holland, and J. Stroeve (2007), Perspectives on the Arctic's shrinking sea-ice cover, *Science*, *315*(5818), 1533–1536, doi:10.1126/science.1139426.
- Simmonds, I. (2015), Comparing and contrasting the behaviour of Arctic and Antarctic sea ice over the 35 year period 1979–2013, *Ann. Glaciol.*, *56*, 18–28, doi:10.3189/2015AoG69A909.
- Simmonds, I., and K. Keay (2009), Extraordinary September Arctic sea ice reductions and their relationships with storm behavior over 1979–2008, *Geophys. Res. Lett.*, *36*, L19715, doi:10.1029/2009GL039810.
- Smedsrud, L. H., R. Ingvaldsen, J. E. Ø. Nilsen, and Ø. Skagseth (2010), Heat in the Barents Sea: Transport, storage, and surface fluxes, *Ocean Sci.*, *6*, 219–234, doi:10.5194/os-6-219-2010.
- Smedsrud, L. H., et al. (2013), The role of the Barents Sea in the Arctic climate system, *Rev. Geophys.*, *51*, 415–449, doi:10.1002/rog.20017.
- Sorteberg, A., and B. Kvingedal (2006), Atmospheric forcing on the Barents Sea winter ice extent, *J. Clim.*, *19*(19), 4772–4784, doi:10.1175/JCLI3885.1.
- Stroeve, J., L. C. Hamilton, C. M. Bitz, and E. Blanchard-Wrigglesworth (2014), Predicting September sea ice: Ensemble skill of the SEARCH Sea Ice Outlook 2008–2013, *Geophys. Res. Lett.*, *41*, 2411–2418, doi:10.1002/2014GL059388.
- Vinje, T. (2001), Anomalies and trends of sea-ice extent and atmospheric circulation in the Nordic Seas during the period 1864–1998, *J. Clim.*, *14*(3), 255–267, doi:10.1175/1520-0442(2001)014<0255:AATOSI>2.0.CO;2.
- Zhang, R. (2015), Mechanisms for low-frequency variability of summer Arctic sea ice extent, *Proc. Natl. Acad. Sci.*, *112*, 4570–4575, doi:10.1073/pnas.1422296112.
- Zhang, X., A. Sorteberg, J. Zhang, R. Gerdes, and J. C. Comiso (2008), Recent radical shifts of atmospheric circulations and rapid changes in Arctic climate system, *Geophys. Res. Lett.*, *35*, L22701, doi:10.1029/2008GL035607.